Cell

JHDM2A, a JmjC-Containing H3K9 Demethylase, Facilitates Transcription Activation by Androgen Receptor

Kenichi Yamane,[1,2] Charalambos Toumazou,[3] Yu-ichi Tsukada,[1,2] Hediye Erdjument-Bromage,[4] Paul Tempst,[4] Jiemin Wong,[3] and Yi Zhang[1,2,*]
[1] Howard Hughes Medical Institute
[2] Department of Biochemistry and Biophysics
Lineberger Comprehensive Cancer Center, University of North Carolina at Chapel Hill, Chapel Hill, NC 27599, USA
[3] Department of Molecular and Cellular Biology, Baylor College of Medicine, One Baylor Plaza, Houston, TX 77030, USA
[4] Molecular Biology Program, Memorial Sloan Kettering Cancer Center, 1275 York Avenue, New York, NY 10021, USA
*Contact: yi_zhang@med.unc.edu
DOI 10.1016/j.cell.2006.03.027

SUMMARY

Covalent modification of histones plays an important role in regulating chromatin dynamics and transcription. Histone methylation was thought to be an irreversible modification until recently. Using a biochemical assay coupled with chromatography, we have purified a JmjC domain-containing protein, JHDM2A, which specifically demethylates mono- and dimethyl-H3K9. Similar to JHDM1, JHDM2A-mediated histone demethylation requires cofactors Fe(II) and α-ketoglutarate. Mutational studies indicate that a JmjC domain and a zinc finger present in JHDM2A are required for its enzymatic activity. Overexpression of JHDM2A greatly reduced the H3K9 methylation level in vivo. Knockdown of JHDM2A results in an increase in the dimethyl-K9 levels at the promoter region of a subset of genes concomitant with decrease in their expression. Finally, JHDM2A exhibits hormone-dependent recruitment to androgen-receptor target genes, resulting in H3K9 demethylation and transcriptional activation. Thus, our work identifies a histone demethylase and links its function to hormone-dependent transcriptional activation.

INTRODUCTION

Posttranslational histone modifications are involved in a variety of cellular processes through regulating chromatin dynamics (Strahl and Allis, 2000). It has become clear that histone methylation is an important part of this histone modification repertoire and functions in heterochromatin formation, X chromosome inactivation, and transcriptional regulation (Margueron et al., 2005; Martin and Zhang, 2005). Histone methylation occurs on both arginine and lysine residues and is catalyzed by three different protein families which include: the protein arginine methyltransferase family, the SET domain-containing family, and the Dot1 protein family (Lachner et al., 2003; Zhang and Reinberg, 2001). While histone arginine methylation generally correlates with transcriptional activation, histone lysine methylation can signal either activation or repression, depending on the particular lysine residue which is methylated (Kouzarides, 2002; Zhang and Reinberg, 2001). Even within the same lysine residue, the biological consequence of methylation can differ depending on the methylation state (Santos-Rosa et al., 2002; Wang et al., 2003).

The steady-state level of histone modification is dictated by the balance between addition and removal of a given modification. While this notion is generally true for acetylation, phosphorylation, and ubiquitylation, early studies looking at the turnover of methyl groups in bulk histones suggested that histone methylation was not reversible since the half-life of histones, and methyl lysine residues within them, were similar (Byvoet, 1972). However, more recent studies indicate that histone methylation is dynamic in certain situations. For example, H3K9 methylation in some inducible inflammatory genes is erased upon activation and restored upon transcriptional repression (Saccani and Natoli, 2002). In addition, trimethyl-H3K27, which is associated with the inactive X chromosome in the trophoblast stem (TS) cells, disappears during TS cell differentiation (Plath et al., 2003; Silva et al., 2003). The first example of an enzyme that was capable of turning over a methylated residue was the human peptidylarginine deiminase 4 (PAD4/PADI4). PAD4/PADI4 converts monomethyl-arginine in histone H3 and H4 to citrulline by demethylimination (Cuthbert et al., 2004; Wang et al., 2004b). However, since PAD4/PADI4 catalyzed demethylimination does not generate arginine and given that PAD4/PADI4 also acts on unmethylated arginine to generate citrulline, PAD4/PADI4 is not a strict demethylase.

A recent study has uncovered a true histone lysine demethylase. Shi and colleagues demonstrated that LSD1/BHC110 can specifically demethylate mono- and dimethyl H3K4 in a FAD (flavin adenine dinucleotide)-dependent oxidative reaction (Shi et al., 2004). Consistent with the notion that H3K4 demethylation participates in transcriptional repression, LSD1 was previously identified in several histone deacetylase complexes (Hakimi et al., 2002; Shi et al., 2003; You et al., 2001). Although there are potential LSD1 homologs in *S. pombe*, no apparent LSD1 homologs exist in *S. cerevisiae* even though at least three distinct lysine residues on H3 can be methylated in this organism. This observation, in combination with the fact that oxidative demethylation catalyzed by the LSD1 family of proteins is unable to demethylate trimethylated lysine residues, raises the possibility that additional demethylases that utilize a different enzymatic mechanisms exist.

In an effort to identify histone demethylases that differ from the LSD1 family of proteins, we have developed an in vitro histone demethylase assay based on the mechanism used by the DNA repair demethylase AlkB (Falnes et al., 2002; Trewick et al., 2002). Using this assay, coupled with chromatography, we have purified and characterized a family of H3K36 demethylases which we have called JHDM1 (JmjC domain-containing histone demethylase 1; Tsukada et al., 2006). In a parallel study, using G9a-methylated histone substrates, we have purified and characterized a second JmjC domain-containing histone demethylase JHDM2A that specifically demethylates H3K9. We demonstrate that the enzymatic activity of JHDM2A depends on an intact JmjC domain and requires cofactors Fe(II) and α-ketoglutarate (α-KG). Although JHDM2A is capable of demethylating mono- and dimethyl-H3K9 in vitro and in vivo, it fails to demethylate trimethyl-H3K9. siRNA-mediated knockdown of JHDM2A results in decreased gene expression concomitant with increased promoter H3K9 methylation. Importantly, JHDM2A interacts directly with androgen receptor (AR) and is recruited to AR target genes in a hormone-dependent manner to mediate transcription activation. Thus, our work identifies a novel histone demethylase and links its function to hormone-dependent transcriptional activation.

RESULTS

Identification of a Histone Demethylase Activity in HeLa Cell Nuclear Extracts

Using a novel biochemical assay, we have recently purified and characterized an H3K36-specific histone demethylase JHDM1A (Tsukada et al., 2006). We demonstrate that JHDM1A-mediated histone demethylation utilizes Fe(II) and α-KG as cofactors generating formaldehyde and succinate and requires the evolutionarily conserved JmjC domain for its activity (Tsukada et al., 2006). In that study, we used SET2-methylated nucleosomal histone substrates to monitor histone demethylase activity. In parallel studies, we also used histone substrates methylated by other histone methyltransferases, including the H3K9 methyltransferase G9a (Tachibana et al., 2002). When the G9a-methylated histone substrates were subjected to demethylation assays using the protein fractions derived from HeLa nuclear extracts (NE) and nuclear pellet (NP; Wang et al., 2001b), we detected a potential H3K9 demethylase activity in the nuclear extract-derived 0.3 M P11 protein fraction (Figure 1A) . To ascertain whether this activity is the result of a genuine demethylase, we examined its dependency on the required cofactors Fe(II) and α-KG. Results shown in Figure 1B demonstrate that release of formaldehyde not only requires the presence of the protein fraction (Figure 1B, compare lanes 1 and 5), but also the cofactors Fe(II) and α-KG (Figure 1B, compare lanes 2 and 3 with lane 1). Addition of ascorbate, which is involved in regenerating Fe(II) from Fe(III), appears to stimulate formaldehyde production (Figure 1B, compare lanes 1 and 4). These results indicate that a histone demethylase activity is present in the nuclear extract-derived 0.3 M P11 fraction and the candidate enzyme likely uses the same oxidative demethylation mechanism used by JHDM1A for histone demethylation (Tsukada et al., 2006).

Purification and Identification of a Histone Demethylase Activity

To identify the protein(s) responsible for this demethylase activity, we monitored the enzymatic activity through five chromatography columns (Figure 2A). After purification of the 0.3 M P11 fraction through DEAE5PW and Phenyl Sepharose columns, we determined that the native mass of the enzymatic activity is about 300 kDa as assessed by a Sephacyl S300 column (Figure 2B). Further purification on a MonoS column allowed us to correlate the enzymatic activity (Figure 2C, bottom panel) to a protein of about 150 kDa, marked by * (Figure 2C, top panel). Because there is a dramatic difference in the enzymatic activities between fractions 17 and 20 (Figure 2C), we concentrated these two fractions and compared their protein composition by SDS-PAGE (Figure 2D). After recovering protein bands unique to fraction 20, they were subjected to mass spectrometry analysis which revealed the protein, marked by *, to be a novel JmjC domain-containing protein named JMJD1A (jumonji domain-containing 1A) or TSGA (testis-specific gene A; Hoog et al., 1991; Figure 2D). To verify that JMJD1A is responsible for the detected demethylase activity, an antibody against this protein was generated and used to immunoprecipitate JMJD1A from the MonoS column fractions 21–29. The immunoprecipitated sample was divided for silver staining, Western blot, and demethylase assays. Results shown in Figure 2E demonstrate that the demethylase activity (bottom panel) was completely depleted from the supernatant (S), which correlates with depletion of the JMJD1A (middle panel). Importantly, silver staining (top panel) revealed a single protein corresponding to JMJD1A. Furthermore, Western blot analysis of the MonoS column fractions demonstrated a perfect correlation between JMJD1A and the enzymatic activity (Figure 2C, bottom two panels). These

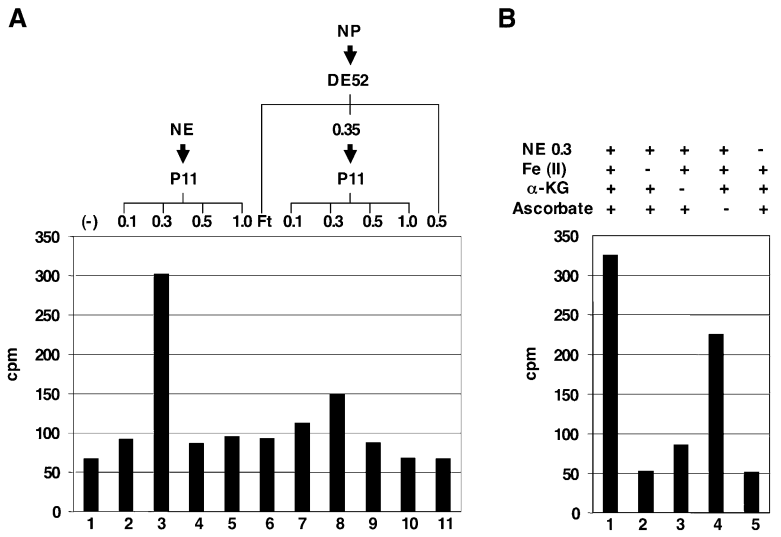

Figure 1. Identification of a Histone Demethylase Activity in HeLa Cells

(A) Histone demethylase activity against G9a-methylated histone substrates was analyzed using P11 column fractions derived from HeLa nuclear extract and nuclear pellet fractions. The numbers above the panel represent the molar concentration of KCl in the elution buffers.

(B) The demethylase activity present in the nuclear extracts of the 0.3 M P11 fraction were dependent on Fe(II) and α-KG.

results collectively suggest that JMJD1A is responsible for the detected demethylase activity. Given that the native size of JMJD1A is about 300 kDa (Figure 2B), it is likely that JMJD1A functions as a homodimer. Because histone demethylase activity is the first identified activity of this protein and that it is the second JmjC domain-containing histone demethylase that we have identified, we have renamed the protein JHDM2A (*J*mjC domain-containing *h*istone *dem*ethylase 2A) to reflect its newly identified function. Accordingly, we have named the other two JHDM2A-related human proteins JHDM2B and JHDM2C, respectively (Figure 3C).

JHDM2A was first identified in a testis cDNA library (Hoog et al., 1991). In situ hybridization studies indicated that JHDM2A is highly expressed in male germ cells, and its steady-state transcript levels are the highest during the meiotic and the postmeiotic stages of germ cell development (Hoog et al., 1991). Domain structure analysis using the SMART program (http://smart.embl-heidelberg.de) revealed the presence of a JmjC domain and a zinc finger (Figure 3A). Given our recent demonstration that JmjC domain is a signature motif for histone demethylases (Tsukada et al., 2006), the presence of a JmjC domain in JHDM2A strongly suggests that JHDM2A is responsible for the detected histone demethylase activity. To directly demonstrate the demethylase activity of JHDM2A, we transfected COS-7 cells with a FLAG-tagged mammalian expression vector. After immunoprecipitation with the anti-FLAG conjugated beads, the immunoprecipitates were split for Western and enzymatic activity assays. Results shown in Figure 3B (lane 1) revealed a robust histone demethylase activity dependent on the FLAG-JHDM2A protein.

To evaluate the importance of the JmjC and the zinc figure domains for the enzymatic activity of JHDM2A, we generated four expression constructs with deletions of the N terminus, zinc finger, N terminus plus zinc finger, and JmjC domain, respectively (Figure 3A). After transfection and immunoprecipitation, these mutant proteins were subjected to Western blotting and demethylase activity assays. Results shown in Figure 3B indicate that both the zinc finger and the JmjC domain are critical for enzymatic activity (Figure 3B, compare lane 1 with lanes 4–6). To further demonstrate the importance of the JmjC domain for enzymatic activity, we generated a single amino acid substitution, H1120Y, in the JmjC domain. We choose to mutate amino acid H1120 because this histidine is highly conserved in the JmjC domain of JHDM2A-related proteins (Figure 3D), and the corresponding histidine in FIH (factor-inhibiting HIF [hypoxia-inducible factor]), a known Fe(II) dependent oxygenase, was found to directly bind to Fe(II) (Elkins et al., 2003). Fe(II) dependency of the histone demethylase activity (Figure 1B) predicts that the H1120Y mutation will disrupt Fe(II) binding and thus impair the enzymatic activity of JHDM2A. Results shown in Figure 3B confirmed this prediction (Figure 3B, compare lanes 1 and 2). The importance of the JmjC and zinc finger for the demethylase activity was also verified in vivo (Figure 5 and see Figure S1 in the Supplemental Data available with this article online). Therefore, we conclude that JHDM2A is a novel histone demethylase and that its JmjC and zinc inger domains are both critical for its enzymatic activity.

JHDM2A Demethylates H3 Mono- and Dimethyl-K9 In Vitro

To further characterize JHDM2A, we generated a baculovirus expressing a FLAG-tagged JHDM2A and purified the protein from infected Sf9 cells by affinity chromatography. After evaluating the purity and quantifying the FLAG-JHDM2A protein (Figure 4A), we analyzed and compared its enzymatic activity with that of the native JHDM2A protein. Results shown in Figure 4B demonstrated that recombinant FLAG-JHDM2A and native JHDM2A have similar activity when equal amounts of proteins are compared (Figure 4B, compare lane 1 with lanes 4 and 5). To analyze

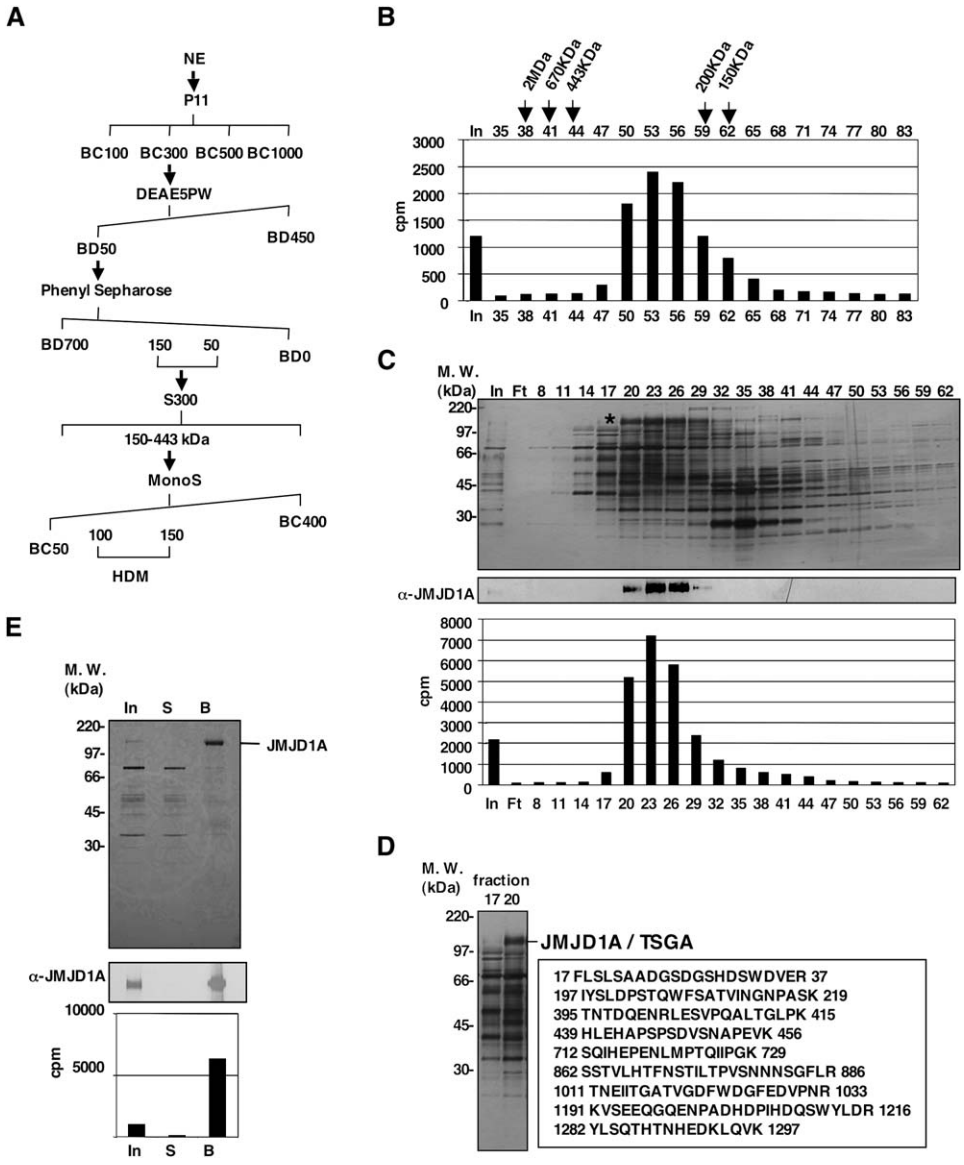

Figure 2. Purification and Identification of a Histone Demethylase Activity

(A) Schematic representation of the steps used to purify the demethylase activity. Numbers represent the salt concentrations (mM) at which the histone demethylase activity elutes from the column.

(B) Histone demethylase activity of the protein fractions derived from a Sephacyl S300 gel-filtration column. The elution profile of the protein markers is indicated on top of the panel.

(C) A silver-stained protein gel (top panel), Western blot (middle panel), and histone demethylase activities (bottom panel) of the protein fractions derived from a MonoS column. A candidate protein that cofractionated with the demethylase activity is indicated by *. The positions of the protein size markers on SDS-PAGE are indicated to the left of the panel.

(D) A silver-stained protein gel comparing the composition of the histone demethylase positive fraction 20 with the adjacent histone demethylase negative fraction 17. The candidate protein was identified by mass spectrometry. A total of 63 peptides covering 53% of the JMJD1A (NP_060903) were identified. Representative peptides identified from mass spectrometry are listed. The numbers correspond to the amino acid numbers of the JMJD1A protein.

(E) Silver-staining (top panel), Western blot (middle panel), and histone demethylase assays (bottom panel) of the immunoprecipitated sample using a JMJD1A antibody. In, S, and B represent input, supernatant, and bound, respectively. The input sample was derived by pooling fractions 21–29 of the MonoS column.

the site specificity of JHDM2A, histone substrates radiolabeled at all known methyl lysine sites in histones H3 (K4, K9, K27, K36, K79) and H4 (K20) were subjected to a demethylation assay containing purified recombinant FLAG-JHDM2A. Of the six substrates, only H3K9 methylated by G9a was a substrate for JHDM2A (Figure 4C). In addition

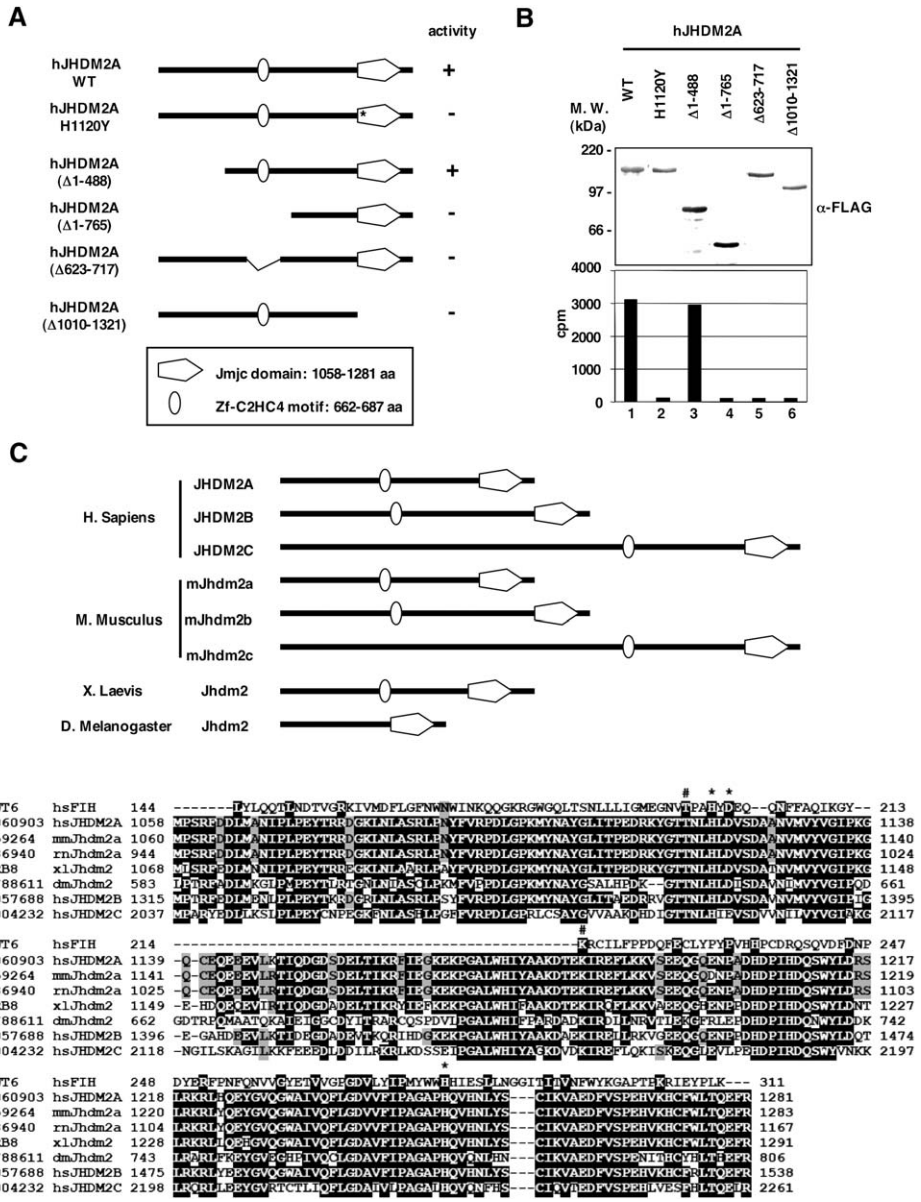

Figure 3. JmjC and Zinc Finger Domains of JHDM2A Are Both Required for Histone Demethylase Activity

(A) Schematic representation of the wild-type and mutant JHDM2A proteins with their activities (right). + represents active and − represents inactive.

(B) Wild-type and mutant FLAG-JHDM1A proteins were expressed in COS-7 cells and immunoprecipitated using a FLAG antibody. The immunoprecipitates were divided for Western blotting (top panel) and demethylase assays (bottom panel).

(C) Diagrammatic representation of the JHDM2 family of proteins from different organisms. Three related proteins were identified in human and mouse, but only one homolog was found in *Drosophila* and *Xenopus*. The JmjC and zinc finger domains present in this family of proteins are shown based on analysis using the SMART program.

(D) Alignment of the JmjC domain of the JHDM2 family members with that of FIH1 using the PAPIA system (www.cbrc.jp/papia/papia.html). The accession number for each of the proteins in the alignment is listed. The numbers represent the amino acid numbers of each protein. The amino acids in FIH1 that are involved in Fe(II) and α-KG binding are indicated by * and #, respectively. Conserved sequences are highlighted with black background.

to H3K9, previous studies indicated that G9a can also methylate H3K27 in vitro (Tachibana et al., 2002). To verify that JHDM2A specifically demethylates H3K9, but not H3K27, we generated radiolabeled substrate histone H3 that contains either a K9R or a K27R mutation using the G9a HMT. In parallel, we also included radiolabeled wild-type recombinant H3 and HeLa core histones in the assay. Results shown in Figure 4D demonstrate that JHDM2A is not able to demethylate H3 when K9 is mutated (Figure 4D, compare lanes 5 and 6), while the K27

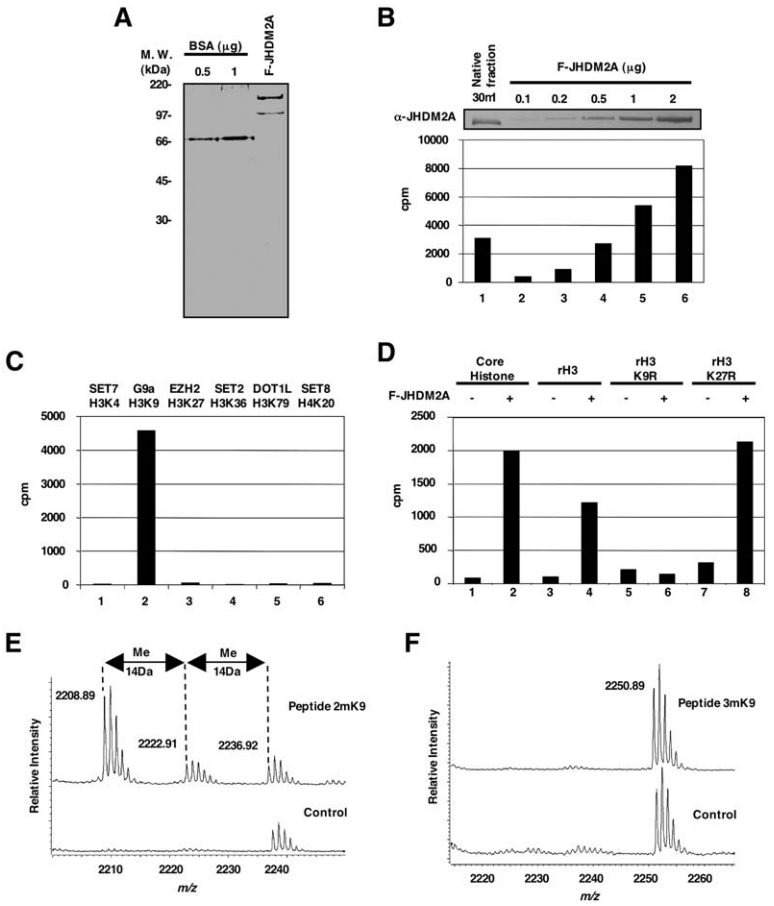

Figure 4. Characterization of the Site and Methylation State Specificity of JHDM2A

(A) A Coomassie-stained protein gel of the purified FLAG-JHDM2A protein expressed in Sf9 cells compared with BSA. The lower band in lane 3 is a degradation product as verified by Western.

(B) Comparable histone demethylase activity of recombinant JHDM2A made in Sf9 cells and the native JHDM2A purified from HeLa cells. Fixed amounts of native JHDM2A were compared with varying amounts of recombinant JHDM2A, quantified by Western blot analysis using JHDM2A antibody (top panel) and histone demethylase activities (bottom panel).

(C) Histone demethylase activity of FLAG-JHDM2A toward equal counts of various methylated histone substrates. Similar results were obtained when equal amounts of substrates in micrograms were used. The histone methyltransferases (HMTs) that were used in generating the various substrates are indicated on top of the panel.

(D) FLAG-JHDM2A demethylates G9a-methylated H3K9, but not H3K27. Native histones purified from HeLa cells and recombinant histone H3, wild-type, or mutant (K9R, K27R), purified from *E. coli*, were methylated by G9a and subjected to demethylase assays in the presence (+) or absence (−) of FLAG-JHDM2A.

(E and F) Mass spectrometry analysis of demethylation of a dimethyl-K9 (E) or a trimethyl-K9 (F) peptide (acetyl-ARTKQTARmeKSTGGKAPRK-biotin) by FLAG-JHDM2A. The enzyme/substrate molar ratio of the reaction is 1:40. Numbers represent the masses of the substrate and product peptides.

mutation does not affect the activity of JHDM2A (Figure 4D, compare lanes 7 and 8). Thus, we conclude that JHDM2A is an H3K9-specific demethylase.

Lysine residues exist in three methylation states (mono-, di-, and trimethylation). To determine whether JHDM2A preferentially demethylates a particular methylation state, we performed a demethylation assay using H3K9-methylated peptide substrates and analyzed demethylation products by mass spectrometry. Results shown in Figure 4E demonstrate that demethylation of a dimethyl-K9 peptide depends on the presence of JHDM2A and generated products with masses that correlate with both monomethyl and unmethylated forms of the peptide, indicating that both mono- and dimethyl-K9 can serve as substrates. In contrast, no demethylation was detected when a trimethyl-K9 peptide that has the same sequence was subjected to parallel analysis (Figure 4F). Based on the above results, we conclude that JHDM2A selectively demethylates H3-mono- and dimethyl-K9.

JHDM2A Demethylates H3 Mono- and Dimethyl-K9 In Vivo

Having demonstrated demethylase activity for JHDM2A in vitro, we sought to test its activity in vivo. To this end, we investigated the effect of overexpression JHDM2A on the H3K9 methylation levels by immunostaining. We find that overexpression of JHDM2A greatly reduced the dimethyl-H3K9 level (Figure 5A). This effect is not simply a result of inaccessibility of modification-specific antibody due to the presence of FLAG-JHDM2A because overexpression of an enzymatically defective mutant did not affect dimethyl-H3K9 levels (Figure 5B). In addition, overexpression of JHDM2A does not alter the expression level of several known H3K9 methyltransferases (Figure S2). A decrease in the level of monomethyl-H3K9 was also observed in cells that overexpress JHDM2A (Figure 5C). However, no effect was observed on the levels of trimethyl-H3K9 (Figures 5D and S3) or dimethyl-H3K27 (Figure 5E). These results indicate that JHDM2A demethylates mono- and dimethyl-H3K9, with a preference for dimethyl-H3K9, in vivo.

JHDM2A Knockdown Leads to Decreased Transcription Concomitant with Increased Promoter H3K9 Dimethylation

Previous studies have linked H3K9 methylation to transcriptional repression and heterochromatin formation (Martin and Zhang, 2005). Therefore, a H3K9 demethylase

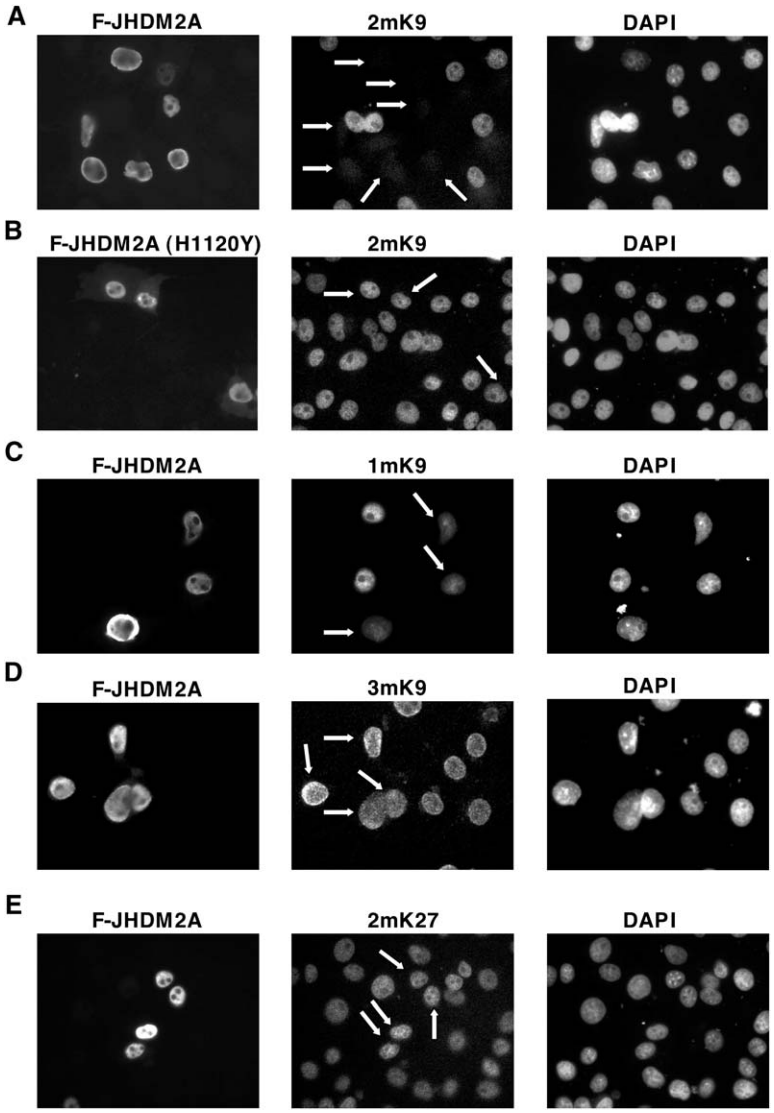

Figure 5. JHDM2A Demethylates Mono- and Dimethyl-H3-K9 In Vivo

COS-7 cells were transfected with wild-type (A, C, D, and E) or mutant (B) FLAG-JHDM2A. Cells were costained with FLAG antibody and different methyl-H3K9 or dimethyl-H3K27 antibodies as indicated in the figure. Arrows point to the transfected cells.

could potentially antagonize gene silencing. To test this possibility, we generated stable Jhdm2a knockdown cells using a vector-mediated RNAi approach (Okada et al., 2005). We choose to perform knockdown in F9 cells because this cell line exhibits the highest Jhdm2a expression in the three cell lines that we have analyzed (Figure 6A). Quantitative PCR (Figure 6B, left panel) and Western blot analysis (Figure 6B, right panel) confirmed that the knockdown efficiency is about 80% at the RNA level and about 70% at the protein level. Compared to the parental F9 cells, no apparent morphological changes were observed in the knockdown cells (data not shown), indicating either that Jhdm2a does not play a critical role in maintaining the undifferentiated state of F9 cells or that the highly related Jhdm2b which is also a H3K9 demethylase expressed in F9 cells (data not shown) may compensate for Jhdm2a function. Although no apparent cell differentiation was observed in response to Jhdm2a knockdown, we have nevertheless analyzed potential changes in expression levels of several differentiation mark genes. The genes that we analyzed include the pluripotency marks (Nanog, Oct4, and Sox2) and differentiation marks (Lamb1, Hoxa1, Hoxb1, and Stra6). Results shown in Figure 6C indicate that, in response to Jhdm2a knockdown, Nanog and Oct4 are down regulated about 20%, while the differentiation marks Lamb1, Hoxb1, and Stra6 are downregulated about 40%–60%. These results are consistent with the notion that Jhdm2a functions as a H3K9 demethylase to positively regulate transcription. In contrast, Hoxa1 expression is upregulated by Jhdm2a knockdown perhaps due to indirect effects (see below).

To investigate whether the observed transcriptional effects due to Jhdm2a knockdown represent a direct effect, we analyzed binding of the JHDM2A protein to the LamB1 and Stra6 promoters by ChIP assay. As a control, we also analyzed its binding to the Hoxa1 gene promoter. Results

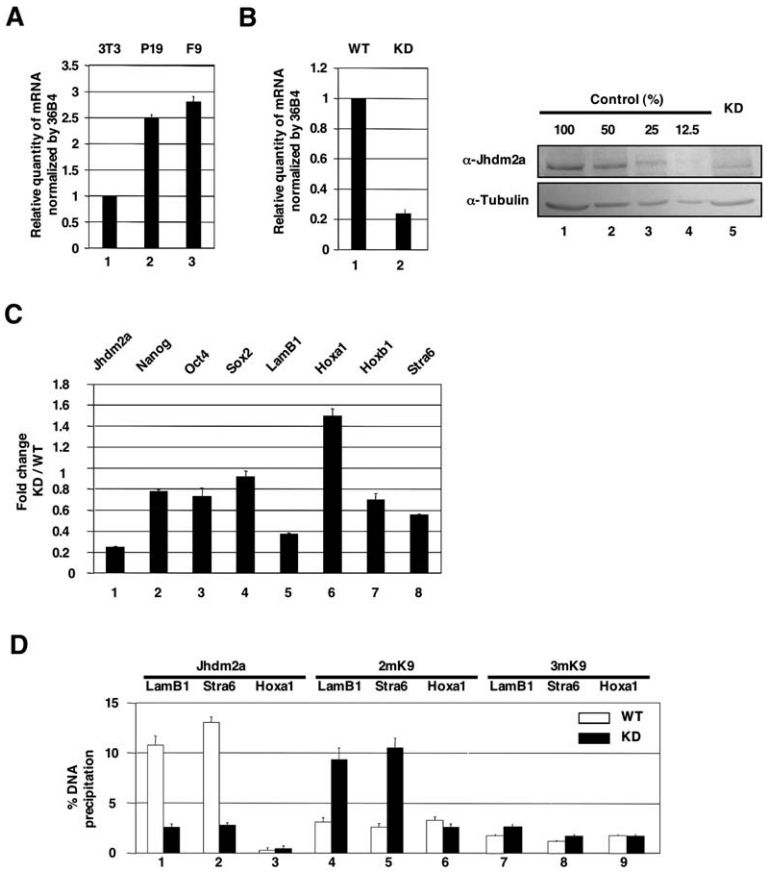

Figure 6. Knockdown of Jhdm2a in F9 Cells Results in Decreased Transcription Concomitant with Increased Promoter H3K9 Dimethylation

(A) Relative expression level of Jhdm2a in NIH3T3, P19, and F9 cells analyzed by quantitative RT-PCR. Data represent average of three independent experiments with error bars.

(B) Characterization of a Jhdm2a knockdown F9 cell line. Quantitative RT-PCR (left panel) and Western blot analysis (right panel) indicates that about 80% knockdown of Jhdm2a at the RNA level and 70% knockdown at the protein level were achieved. Data represent average of three independent experiments with error bars.

(C) Quantitative RT-PCR analysis of changes in RNA level of several pluripotency and differentiation marker genes in response to Jhdm2a knockdown. The changes are expressed as the ratio of the expression level in knockdown cells to that of the wild-type control. Data represent average of three independent experiments with error bars.

(D) Q-PCR results of ChIPed DNA in control (open bars) and Jhdm2a knockdown (filled bars) cells. The gene promoters analyzed and the antibodies used for ChIP are indicated. All Q-PCR have been repeated three times. The average with standard deviation is presented. Data represent average of three independent experiments with error bars.

shown in Figure 6D indicate that JHDM2A binds to the LamB1 and Stra6 promoters, but not the Hoxa1 promoter (Figure 6D, compare columns 1 and 2 with 3). Knockdown of Jhdm2a significantly decreased JHDM2A binding, indicating the detected ChIP signals are specific (Figure 6D, columns 1 and 2). Consistent with the observation that JHDM2A functions as a dimethyl-K9 demethylase, knockdown Jhdm2a increased the dimethyl-K9 levels at the LamB1 and Stra6 promoters but had little effect on the Hoxa1 promoter (Figure 6D, columns 4–6). Consistent with the fact that Jhdm2a is a dimethyl-K9-specific demethylase, knockdown Jhdm2a did not cause a significant alteration in the trimethyl-K9 levels on any of the three promoters analyzed (Figure 6D, columns 7–9). Based on these results, we conclude that JHDM2A is targeted to a subset of genes to demethylate dimethyl-K9 and positively regulate expression of these genes.

JHDM2A-Mediated H3K9 Demethylation Contributes to Hormone-Dependent AR Activation

JHDM2A has two closely related homologs, JHDM2B and JHDM2C (Figure 3C). Interestingly, JHDM2C was first identified in a yeast two-hybrid screen as a thyroid hormone receptor (TR)-interacting protein named TRIP8 (Lee et al., 1995). In addition, JHDM2A contains an ^{885}LXXLL^{889} sequence, which is a signature motif involved in nuclear hormone-receptor interaction (Heery et al., 1997). These observations prompted us to test for potential involvement of JHDM2A in transcriptional regulation by nuclear receptors. While we failed to detect a hormone-dependent interaction with TR by both in vitro pull-down and coimmunoprecipitation assays (data not shown), we found that JHDM2A interacted with androgen receptor (AR) in a ligand-dependent manner (Figure 7A). To investigate the in vivo relevance of this in vitro interaction, we asked whether JHDM2A is recruited to known AR target genes in a hormone-dependent manner. Thus, we performed ChIP assays on two well-characterized AR target genes, PSA and NKX3.1, in LNCaP cells in the presence or absence of hormone. Results shown in Figure 7B demonstrated a strong binding of the AR to the PSA enhancer upon R1881 treatment (Figure 7B, third panel, compare lanes 1 and 2). Similarly, strong hormone-dependent binding of the AR to a region containing a functional ARE (AR enhancer) located ~3 kb upstream of the NKX3.1 transcriptional start site was also detected (Figure 7B, third panel, compare lanes 3 and 4). Consistent with hormone-induced transcriptional activation (data not shown), an increase in histone acetylation was detected in both cases (Figure 7B, fourth panel). Importantly, R1881 treatment also led to increased association of JHDM2A with AR target genes (Figure 7B, fifth panel), concomitant

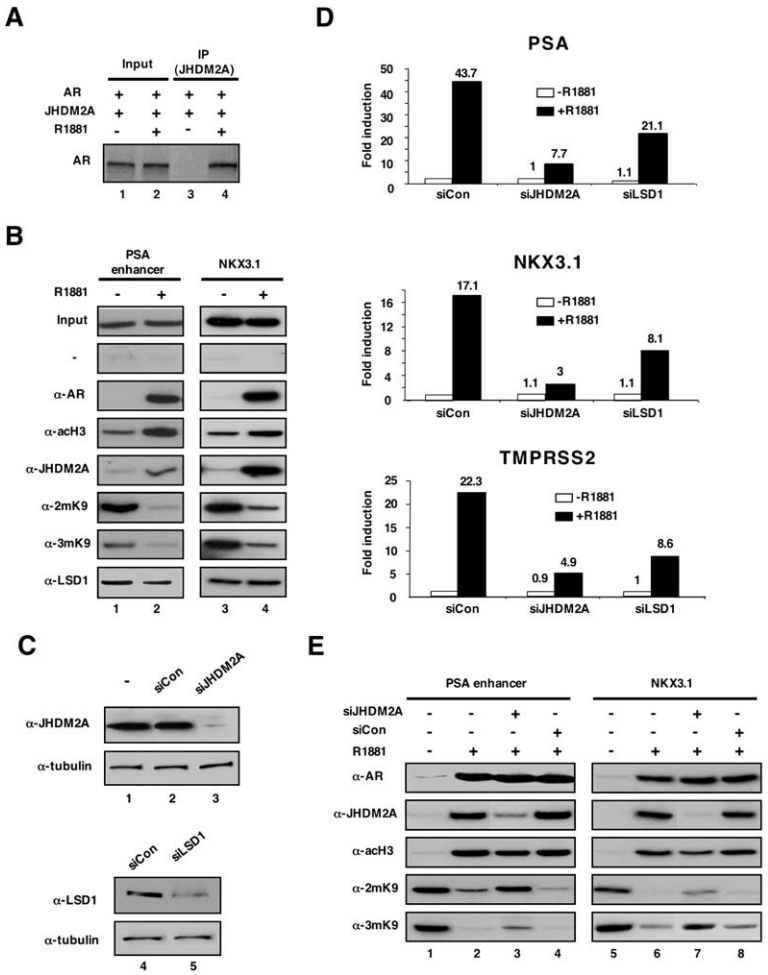

Figure 7. JHDM2A Functions as a Coactivator for AR and Is Required for Hormone-Induced H3K9 Demethylation

(A) JHDM2A interacts with AR in a hormone-dependent manner in vitro. Recombinant JHDM2A was mixed with in vitro translated ^{35}S-labeled AR in the absence or presence of R1881 (100 nM). After immunoprecipitation with anti-JHDM2A antibody, AR was detected by autoradiography.

(B) Hormone-dependent recruitment of JHDM2A to the PSA and NKX3.1 enhancers in vivo. LNCaP cells were cultured in charcoal-stripped serum medium for 3 days and then treated without or with R1881 (50 nM) for 1 hr before processing for ChIP assays.

(C) Knockdown of JHDM2A and LSD1 in LNCaP cells by siRNA. LNCaP cells were transfected with a scramble (siCon), siJHDM2A, or siLSD1 as indicated. Tubulin serves as a loading control.

(D) Quantitative RT-PCR analysis showing the effect of JHDM2A or LSD1 knockdown on R1881-dependent activation of three AR target genes. The cells were treated as in (B) except the cells were collected for RNA isolation 8 hr after the R1881 treatment.

(E) Knockdown of JHDM2A impaired hormone-induced H3K9 demethylation. The LNCaP cells were treated with siJHDM2A or siCon for 3 days and then 50 nM R1881 for 1 hr before processed for ChIP assays using antibodies as indicated.

with decreases in the level of dimethyl- and trimethyl-H3K9 (Figure 7B, sixth and seventh panels). In contrast to JHDM2A, which binds to PSA and NKX3.1 genes in a hormone-dependent manner, association of LSD1 with these two genes was not affected by hormone treatment (Figure 7B, last panel), consistent with a previous report (Metzger et al., 2005).

To directly test and compare the role of JHDM2A and LSD1 in hormone-dependent transcriptional activation, we used siRNA to knockdown JHDM2A and LSD1 in LNCaP cells (Figure 7C). We then evaluated the effects of JHDM2A or LSD1 knockdown on the hormone-induced activation of three AR target genes, PSA, NKX3.1, and TMPRSS22, by quantitative RT-PCR. Results shown in Figure 7D demonstrate that while treatment with R1881 for 8 hr robustly activated transcription from all three AR target genes, knockdown of JHDM2A led to significant reduction in hormone response. Although knockdown of LSD1 also led to reduced hormone response, the effect is not as significant in comparison with knockdown of JHDM2A. Thus, we conclude that JHDM2A is critically important for optimal hormone-dependent transcriptional activation by AR.

To evaluate whether JHDM2A is important for the hormone-induced H3K9 demethylation observed above (Figure 7B), we performed JHDM2A knockdown in LNCaP cells followed by treatment with R1881 for 1 hr before ChIP analysis. Results shown in Figure 7E demonstrate that the hormone-induced recruitment of JHDM2A to the PSA enhancer and NKX3.1 gene was largely abrogated upon siJHDM2A treatment (Figure 7E, second panel, compare lane 3 with lanes 2 and 4; compare lane 7 with lanes 6 and 8). Importantly, knockdown of JHDM2A significantly impaired the hormone-induced reduction of dimethyl-H3K9 at the PSA enhancer (Figure 7E, fourth panel, compare lanes 2 and 3). Although to a lesser extent, knockdown of JHDM2A also affected the hormone-induced reduction of dimethyl-H3K9 at NKX3.1 (Figure 7E, fourth panel, compare lanes 6 and 7). These results indicate that JHDM2A is required for efficient demethylation of repressive dimethyl-H3K9 at AR target genes. Interestingly, although JHDM2A has no activity toward trimethyl-H3K9 (Figures 4F, 5D, 6D, and S3C), knockdown of JHDM2A also affected hormone-induced reduction of trimethyl-H3K9 for both PSA enhancer and NKX3.1 (Figure 7E, last panel). Whether the observed effects on

trimethyl-H3K9 are direct or indirect remains to be determined. It is interesting to note that knockdown of JHDM2A also appears to reduce the hormone-induced H3 acetylation levels (Figure 7E, third panel, compare lanes 2 and 3, 6 and 7). One explanation for this observation is that H3K9 demethylation is a prerequisite for H3K9 acetylation. On the other hand, knockdown of JHDM2A did not affect hormone-induced binding of AR to both target genes (Figure 7E, first panel), suggesting that JHDM2A contributes to AR-mediated transcription activation subsequent to its binding to target genes.

Previous studies indicate that LSD1 is also capable of catalyzing dimethyl-H3K9 demethylation when it associates with AR (Metzger et al., 2005). To determine whether LSD1 is required for hormone-dependent association of JHDM2A with AR target genes, we analyzed occupancy of JHDM2A and dimethyl-H3K9 levels of the PSA enhancer with or without LSD1 knockdown. Results shown in Figure S4 demonstrate that knockdown of LSD1 affected neither the binding of AR to the PSA enhancer nor the hormone-induced recruitment of JHDM2A. However, knockdown of LSD1 did partially impair the hormone-induced reduction of dimethyl-H3K9. This result and the results shown in Figure 7 collectively indicate that both JHDM2A and LSD1 contribute to hormone-induced demethylation of dimethyl-H3K9 of the PSA enhancer.

DISCUSSION

Using a histone demethylase assay (Tsukada et al., 2006), we purified and characterized a new H3K9 demethylase, JHDM2A, that specifically targets mono- and dimethyl H3K9 for demethylation. Consistent with the notion that H3K9 methylation is involved in transcriptional repression, JHDM2A-mediated H3K9 demethylation plays an important role in hormone-dependent AR activation.

Multiple Mechanisms Are Employed to Remove Methyl Groups on Histones

Histone methylation was originally thought to be a "permanent" modification. Before an enzyme capable of removing methyl groups was identified, at least two models were proposed to explain the turnover of methyl groups on histone molecules. The first model involved histone tail clipping (Allis et al., 1980), while the second model involved replacement of methylated histone with a variant histone (Ahmad and Henikoff, 2002). Recent studies indicate that enzyme-catalyzed turnover of methyl groups on histone is more prominent than was originally thought. For example, PAD4/PADI4 can convert monomethyl arginines on histone H3 and H4 to citrulline by demethylimination (Cuthbert et al., 2004; Wang et al., 2004b). LSD1, a member of the amine oxidase family, has been recently shown to catalyze demethylation of mono- and dimethyl-H3K4 through a FAD-dependent oxidative reaction (Shi et al., 2004). Using an unbiased biochemical assay (Tsukada et al., 2006), we have successfully purified and characterized two distinct histone demethylases, JHDM1A and JHDM2A, that target different lysine residues of histone H3 for demethylation. Interestingly, both demethylases contain an evolutionarily conserved JmjC domain and require Fe(II) and α-KG as cofactors. Thus, at least two families of proteins, the amine oxidase family and the JmjC domain-containing family, can convert methyl lysine to lysine.

The chemical nature of the amine oxidation reaction prevents the LSD1 family of demethylases from catalyzing the removal of trimethyl lysine, since this reaction requires a protonated nitrogen (Bannister et al., 2002). However, the JmjC domain-containing proteins, which use an oxidative hydroxylation mechanism for histone demethylation (Trewick et al., 2005), do not have such a limitation. Surprisingly, JHDM1A and JHDM2A can only demethylate mono- and dimethyl lysine. The fact that both JmjC family of histone demethylases that we identified (JHDM1 and JHDM2) act only on mono- and dimethyl lysine, does not mean that the trimethyl state is irreversible. Instead, we believe our observation is simply a reflection of the nature of the substrates that we have used in the purification of these two enzymes. In vitro, both Set2 and G9a predominantly methylate lysine residues to dimethyl state. Consistent with this rationale, we have successfully identified JHDM3, a novel histone demethylase capable of demethylating trimethyl-H3K9 and trimethyl-H3K36 (R. Klose, K.Y., and Y.Z., unpublished data). Therefore, JmjC domain-containing proteins are capable of demethylating all the three methyl lysine states.

Both JHDM1A and JHDM2A exhibit striking substrate specificity. They not only selectively demethylate a single lysine residue but also demethylate particular lysine states. We speculate that the site specificity is likely determined by interactions between the amino acids adjacent to the lysine residues on histones and the catalytic domain of the enzyme. The methylation state specificity may be determined by the size of the catalytic site, analogous to the situation observed for SET domain histone methyltransferases. If the catalytic site of these histone demethylases is spatially constrained, it is possible that they are unable to accommodate a trimethyl lysine residue. Structural studies are required to clarify these predictions. The striking specificity of these histone demethylases suggests a large number of demethylases are required to satisfy the diverse range of enzymatic requirements and counteract histone methylation. The LSD1 family has about ten related proteins and only a few are potential histone demethylases (Kubicek and Jenuwein, 2004). Although more than 30 JmjC domain-containing proteins exist in mammals, the amino acids predicted to bind cofactors are not conserved in many of these proteins (K.Y. and Y.Z., unpublished data). In addition, some of the predicted demethylases are likely to target none histone proteins as substrates. Furthermore, enzymes capable of directly removing methyl groups from methylarginine remain to be identified. Therefore, histone demethylases that do not belong to the LSD1 or the JmjC families are likely to be discovered.

JHDM2A Functions as a Coactivator for AR

JHDM2A was initially cloned as a male germ cell-specific gene from rat (Hoog et al., 1991). In situ hybridization studies indicate that JHDM2A is mainly expressed in male germ cells and the steady-state transcript levels are highest during the meiotic and postmeiotic stages of germ cell development (Hoog et al., 1991). This indicates that JHDM2A may have a role in male germ cell development. Interestingly, rapid turnover of H3K9 methylation has been observed during germ cell development (Morgan et al., 2005; Seki et al., 2005). Whether JHDM2A is responsible for this rapid turnover remains to be determined. Consistent with the observation that JHDM2A is highly expressed in male germ cells, we found that JHDM2A is highly expressed in the F9 embryonic carcinoma cells derived from testis. ChIP analysis indicates that JHDM2A is bound to promoters of several differentiation-associated genes, where it maintains low levels of expression in the undifferentiated state. These genes include LamininB1 and Stra6 (Figure 6). LamininB1 is an important component of the extracellular matrix, but recent studies indicate that it also facilitates germ cell movement (Siu and Cheng, 2004). Stra6 is a membrane protein expressed in the Sertoli cells of the testis and is regulated in a spermatogenic cycle-dependent manner (Bouillet et al., 1997). Thus, involvement of JHDM2A in LamininB1 and Stra6 expression points to a function for JHDM2A in male germ cell development.

In addition to the constitutive binding and function in maintaining gene expression observed in F9 cells, JHDM2A also responds to hormone treatment during upregulation of AR target genes. Our finding that JHDM2A interacts with liganded AR in vitro and is recruited to the PSA and NKX3.1 enhancers in a ligand-dependent manner in LNCaP cells suggests JHDM2A likely functions as a transcriptional coactivator for AR (Figure 7B). Indeed, using a siRNA-mediated knockdown approach, we confirmed that JHDM2A is required for optimal transcriptional activation of all three AR target genes we have tested (Figure 7D). Consistent with a previous report (Metzger et al., 2005), we confirmed that knockdown of LSD1 affects transcriptional activation by AR. Importantly, knockdown of JHDM2A or LSD1 impairs hormone-induced reduction of dimethyl-H3K9 (Figures 7E and S4), thus providing strong evidence that JHDM2A and LSD1 both participate in the demethylation of the PSA enhancer in response to hormone treatment. Since knockdown of JHDM2A or LSD1 does not affect AR binding, our data suggest that demethylation of H3K9 is required for a subsequent step(s) in hormone-dependent transcriptional activation. Because JHDM2A is unable to remove trimethyl-K9, we suspect that the effect of JHDM2A knockdown on trimethyl-H3K9 could be indirect. Although unlikely, we cannot rule out the possibility that JHDM2A may be able to demethylate trimethyl-H3K9 once targeted to chromatin by AR. In this regard, LSD1 was shown to convert from a H3K4 demethylase to a H3K9 demethylase when associated with AR (Metzger et al., 2005). The demonstration of the involvement of JHDM2A in transcriptional activation by AR suggests that JHDM2A likely has a widespread role in transcriptional regulation.

EXPERIMENTAL PROCEDURES

Histone Demethylase Assay, Protein Identification, and Mass Spectrometry

The histone demethylase assay was performed essentially as previously described (Tsukada et al., 2006). A detailed description can be found in Supplemental Experimental Procedures. For protein identification, the candidate polypeptide was digested with trypsin, and the protein was identified as previously described (Wang et al., 2004a). For peptide substrate analysis, an aliquot (1 μl) of the demethylation reaction mixture was diluted 100-fold with 0.1% formic acid and loaded onto a 2 μl bed volume of Poros 50 R2 (PerSeptive Biosystems) reversed-phase beads packed into an Eppendorf gel-loading tip. The peptides were eluted with 5 μl of 30% acetonitrile/0.1% formic acid. A fraction (0.5 ml) of this peptide pool was analyzed by matrix-assisted laser-desorption/ionization (MALDI) time-of-flight (TOF) mass spectrometry (MS), using a BRUKER UltraFlex TOF/TOF instrument (Bruker Daltonics) as described (Erdjument-Bromage et al., 1998).

Constructs and Antibodies

Plasmids encoding GST-SET7, GST-SET8, GST-hDOT1L (1–416), and components of the EZH2 complex have been previously described (Cao and Zhang, 2004; Min et al., 2003; Wang et al., 2001a, 2001b). Plasmids encoding GST-G9a (621–1000), and CBP-Set2-FLAG (*S. pombe*) were kindly provided by Drs. Shinkai, and Strahl, respectively. A plasmid encoding hJHDM2A was constructed by PCR amplification from a human KIAA clone (KIAA 0742) and was inserted into XhoI sites of an N-terminal FLAG-tagged pcDNA3 vector or an N-terminal FLAG-tagged pFASTBAC vector. pcDNA3-FLAG-JHDM2A (H1120Y) and deletion mutants (489–1321 aa, 766–1321 aa, 1–1009 aa, and Δ623–717) were generated by PCR. All the constructs generated through PCR were verified by sequencing. RNAi constructs were made by synthesizing oligonucleotides encoding 19 bp short-hairpin RNA that target mJhdm2a (RNAi1, 5′-GTACAAGAAGCAGTAATAA-3′; RNAi2, 5′-AGGTGTCACTAGCCTTAAT-3′) and cloned into pMSCVneo retrovirus vector (Clonetech) under the regulation of H1 RNA promoter as described previously (Okada et al., 2005).

The sources of the antibodies used are as follows: H3 trimethyl-K4 (Abcam 8580), H3 monomethyl-K9 (Abcam 9045), H3 dimethyl-K9 (Upstate 07-411), and H3 dimethyl-K27 (Upstate 07-452). H3 trimethyl-K9 antibody has been previously described (Plath et al., 2003). The AR (N-20) antibody and acH3 antibody were purchased from Santa Cruz and Upstate, respectively. The antibody against FLAG and secondary antibodies for immunofluorescence were purchased from Sigma and Jackson ImmunoResearch Laboratories, respectively. Antibodies against hJHDM2A were generated in rabbits using the first 495 amino acids of the protein as antigen.

Immunostaining

COS-7 and NIH3T3 cells were plated onto glass coverslips in a 12-well plate and cultured for 1 day. Cells were transiently transfected with plasmids by FuGene6. Two days after transfection, cells were washed with PBS and fixed in 4% paraformaldehyde for 10 min. The cells were then washed three times with cold PBS and permeabilized for 5 min with cold PBS containing 0.2% Triton X-100. Permeabilized cells were then washed three times with blocking buffer (1% bovine serum albumin in PBS) and blocked for 30 min before incubation with primary antibodies for 1 hr in a humidified chamber. After three consecutive 5 min washes with PBS, cells were incubated with secondary antibodies for 1 hr before being washed with PBS and stained with 4,6-diamidino-2-phenylindole dihydrochloride (DAPI) in PBS. Cells were washed again twice with PBS and then mounted in fluorescent

mounting medium (Dako) before viewing under a Zeiss immunofluorescence microscope.

Generation of a Stable JHDM2A Knockdown Cell Line

F9 cells were cultured in DMEM media supplied with 10% FBS on 0.1% gelatin-coated plates. The MSCVneo-JHDM2A siRNA vector was cotransfected with pGag-pol and pVSVG into 293T cells by calcium-phosphate mediated transfection. At 48 to 72 hr posttransfection, the supernatants were collected and were used for transduction of F9 cells by spinoculation. Stable transfectants were selected in the presence of 500 μg/ml G418 (Gibco). Cells derived from these transfectants were used for Western blotting, real-time PCR, and ChIP analysis.

AR-JHDM2A Interaction

The in vitro translated ^{35}S-methionine labeled AR (10 μl) was mixed with 3 μl (300 ng) of purified recombinant JHDM2A in binding buffer (20 mM HEPES [pH7.6], 50 mM KCl, 1 mM DTT, 0.5 mM PMSF, and 10% glycerol) in the presence or absence of 100 nM R1881 in a 100 μl reaction and rotated in the cold room for 2 hr. Protein A agarose beads and anti-JHDM2A antibody (10 μl) were then added and incubated for 1 hr. After extensive washing with the binding buffer, the AR was resolved by a 10% SDS-PAGE and visualized by autoradiography.

Procedures for purification of the native and recombinant JHDM2A, real-time PCR, and ChIP assays can be found in Supplemental Experimental Procedures.

Supplemental Data

Supplemental Data include four figures and Supplemental Experimental Procedures and can be found with this article online at http://www.cell.com/cgi/content/full/125/3/483/DC1/.

ACKNOWLEDGMENTS

We thank Lynne Lacomis for help with mass spectrometry; B. Strahl, Y. Shinkai, K. Miyazono for Set2, G9a, and pcDNA3-FLAG constructs; Mark Bedford for peptides; R. Cao for the EZH2 complex; Y. Okada for advice on F9 cell transduction; David Leonard in qPCR analysis and Michele Barton for siLSD1; and R. Klose for critical reading of the manuscript. This work was supported by NIH grant GM68804 (to Y.Z.), P30 CA08748 (to P.T.), and DK065264 and DAMD17-03-1-0165 (to J.W.). Y.Z. is an Investigator of the Howard Hughes Medical Institute.

Received: December 15, 2005
Revised: February 13, 2006
Accepted: March 23, 2006
Published online: April 6, 2006

REFERENCES

Ahmad, K., and Henikoff, S. (2002). The histone variant H3.3 marks active chromatin by replication-independent nucleosome assembly. Mol. Cell *9*, 1191–1200.

Allis, C.D., Bowen, J.K., Abraham, G.N., Glover, C.V., and Gorovsky, M.A. (1980). Proteolytic processing of histone H3 in chromatin: A physiologically regulated event in *Tetrahymena* micronuclei. Cell *20*, 55–64.

Bannister, A.J., Schneider, R., and Kouzarides, T. (2002). Histone methylation: Dynamic or static? Cell *109*, 801–806.

Bouillet, P., Sapin, V., Chazaud, C., Messaddeq, N., Decimo, D., Dolle, P., and Chambon, P. (1997). Developmental expression pattern of Stra6, a retinoic acid-responsive gene encoding a new type of membrane protein. Mech. Dev. *63*, 173–186.

Byvoet, P. (1972). In vivo turnover and distribution of radio-N-methyl in arginine-rich histones from rat tissues. Arch. Biochem. Biophys. *152*, 887–888.

Cao, R., and Zhang, Y. (2004). SUZ12 is required for both the histone methyltransferase activity and the silencing function of the EED-EZH2 complex. Mol. Cell *15*, 57–67.

Cuthbert, G.L., Daujat, S., Snowden, A.W., Erdjument-Bromage, H., Hagiwara, T., Yamada, M., Schneider, R., Gregory, P.D., Tempst, P., Bannister, A.J., and Kouzarides, T. (2004). Histone deimination antagonizes arginine methylation. Cell *118*, 545–553.

Elkins, J.M., Hewitson, K.S., McNeill, L.A., Seibel, J.F., Schlemminger, I., Pugh, C.W., Ratcliffe, P.J., and Schofield, C.J. (2003). Structure of factor-inhibiting hypoxia-inducible factor (HIF) reveals mechanism of oxidative modification of HIF-1 alpha. J. Biol. Chem. *278*, 1802–1806.

Erdjument-Bromage, H., Lui, M., Lacomis, L., Grewal, A., Annan, R.S., McNulty, D.E., Carr, S.A., and Tempst, P. (1998). Examination of micro-tip reversed-phase liquid chromatographic extraction of peptide pools for mass spectrometric analysis. J. Chromatogr. A. *826*, 167–181.

Falnes, P.O., Johansen, R.F., and Seeberg, E. (2002). AlkB-mediated oxidative demethylation reverses DNA damage in Escherichia coli. Nature *419*, 178–182.

Hakimi, M.A., Bochar, D.A., Chenoweth, J., Lane, W.S., Mandel, G., and Shiekhattar, R. (2002). A core-BRAF35 complex containing histone deacetylase mediates repression of neuronal-specific genes. Proc. Natl. Acad. Sci. USA *99*, 7420–7425.

Heery, D.M., Kalkhoven, E., Hoare, S., and Parker, M.G. (1997). A signature motif in transcriptional co-activators mediates binding to nuclear receptors. Nature *387*, 733–736.

Hoog, C., Schalling, M., Grunder-Brundell, E., and Daneholt, B. (1991). Analysis of a murine male germ cell-specific transcript that encodes a putative zinc finger protein. Mol. Reprod. Dev. *30*, 173–181.

Kouzarides, T. (2002). Histone methylation in transcriptional control. Curr. Opin. Genet. Dev. *12*, 198–209.

Kubicek, S., and Jenuwein, T. (2004). A crack in histone lysine methylation. Cell *119*, 903–906.

Lachner, M., O'Sullivan, R.J., and Jenuwein, T. (2003). An epigenetic road map for histone lysine methylation. J. Cell Sci. *116*, 2117–2124.

Lee, J.W., Choi, H.S., Gyuris, J., Brent, R., and Moore, D.D. (1995). Two classes of proteins dependent on either the presence or absence of thyroid hormone for interaction with the thyroid hormone receptor. Mol. Endocrinol. *9*, 243–254.

Margueron, R., Trojer, P., and Reinberg, D. (2005). The key to development: interpreting the histone code? Curr. Opin. Genet. Dev. *15*, 163–176.

Martin, C., and Zhang, Y. (2005). The diverse functions of histone lysine methylation. Nat. Rev. Mol. Cell Biol. *6*, 838–849.

Metzger, E., Wissmann, M., Yin, N., Muller, J.M., Schneider, R., Peters, A.H., Gunther, T., Buettner, R., and Schule, R. (2005). LSD1 demethylates repressive histone marks to promote androgen-receptor-dependent transcription. Nature *437*, 436–439.

Min, J., Zhang, Y., and Xu, R.M. (2003). Structural basis for specific binding of Polycomb chromodomain to histone H3 methylated at Lys 27. Genes Dev. *17*, 1823–1828.

Morgan, H.D., Santos, F., Green, K., Dean, W., and Reik, W. (2005). Epigenetic reprogramming in mammals. Hum. Mol. Genet. *14 Spec No 1*, R47–R58.

Okada, Y., Feng, Q., Lin, Y., Jiang, Q., Li, Y., Coffield, V.M., Su, L., Xu, G., and Zhang, Y. (2005). hDOT1L links histone methylation to leukemogenesis. Cell *121*, 167–178.

Plath, K., Fang, J., Mlynarczyk-Evans, S.K., Cao, R., Worringer, K.A., Wang, H., de la Cruz, C.C., Otte, A.P., Panning, B., and Zhang, Y.

(2003). Role of histone H3 lysine 27 methylation in X inactivation. Science *300*, 131–135.

Saccani, S., and Natoli, G. (2002). Dynamic changes in histone H3 Lys 9 methylation occurring at tightly regulated inducible inflammatory genes. Genes Dev. *16*, 2219–2224.

Santos-Rosa, H., Schneider, R., Bannister, A.J., Sherriff, J., Bernstein, B.E., Emre, N.C., Schreiber, S.L., Mellor, J., and Kouzarides, T. (2002). Active genes are tri-methylated at K4 of histone H3. Nature *419*, 407–411.

Seki, Y., Hayashi, K., Itoh, K., Mizugaki, M., Saitou, M., and Matsui, Y. (2005). Extensive and orderly reprogramming of genome-wide chromatin modifications associated with specification and early development of germ cells in mice. Dev. Biol. *278*, 440–458.

Shi, Y., Sawada, J., Sui, G., Affar, E.B., Whetstine, J.R., Lan, F., Ogawa, H., Luke, M.P., Nakatani, Y., and Shi, Y. (2003). Coordinated histone modifications mediated by a CtBP co-repressor complex. Nature *422*, 735–738.

Shi, Y., Lan, F., Matson, C., Mulligan, P., Whetstine, J.R., Cole, P.A., Casero, R.A., and Shi, Y. (2004). Histone demethylation mediated by the nuclear amine oxidase homolog LSD1. Cell *119*, 941–953.

Silva, J., Mak, W., Zvetkova, I., Appanah, R., Nesterova, T.B., Webster, Z., Peters, A.H., Jenuwein, T., Otte, A.P., and Brockdorff, N. (2003). Establishment of histone h3 methylation on the inactive x chromosome requires transient recruitment of eed-enx1 polycomb group complexes. Dev. Cell *4*, 481–495.

Siu, M.K., and Cheng, C.Y. (2004). Dynamic cross-talk between cells and the extracellular matrix in the testis. Bioessays *26*, 978–992.

Strahl, B.D., and Allis, C.D. (2000). The language of covalent histone modifications. Nature *403*, 41–45.

Tachibana, M., Sugimoto, K., Nozaki, M., Ueda, J., Ohta, T., Ohki, M., Fukuda, M., Takeda, N., Niida, H., Kato, H., and Shinkai, Y. (2002). G9a histone methyltransferase plays a dominant role in euchromatic histone H3 lysine 9 methylation and is essential for early embryogenesis. Genes Dev. *16*, 1779–1791.

Trewick, S.C., Henshaw, T.F., Hausinger, R.P., Lindahl, T., and Sedgwick, B. (2002). Oxidative demethylation by Escherichia coli AlkB directly reverts DNA base damage. Nature *419*, 174–178.

Trewick, S.C., McLaughlin, P.J., and Allshire, R.C. (2005). Methylation: lost in hydroxylation? EMBO Rep. *6*, 315–320.

Tsukada, Y., Fang, J., Erdjument-Bromage, H., Warren, M.E., Borchers, C.H., Tempst, P., and Zhang, Y. (2006). Histone demethylation by a family of JmjC domain-containing proteins. Nature *439*, 811–816.

Wang, H., Cao, R., Xia, L., Erdjument-Bromage, H., Borchers, C., Tempst, P., and Zhang, Y. (2001a). Purification and functional characterization of a histone H3-lysine 4-specific methyltransferase. Mol. Cell *8*, 1207–1217.

Wang, H., Huang, Z.Q., Xia, L., Feng, Q., Erdjument-Bromage, H., Strahl, B.D., Briggs, S.D., Allis, C.D., Wong, J., Tempst, P., and Zhang, Y. (2001b). Methylation of histone H4 at arginine 3 facilitating transcriptional activation by nuclear hormone receptor. Science *293*, 853–857.

Wang, H., An, W., Cao, R., Xia, L., Erdjument-Bromage, H., Chatton, B., Tempst, P., Roeder, R.G., and Zhang, Y. (2003). mAM facilitates conversion by ESET of dimethyl to trimethyl lysine 9 of histone H3 to cause transcriptional repression. Mol. Cell *12*, 475–487.

Wang, H., Wang, L., Erdjument-Bromage, H., Vidal, M., Tempst, P., Jones, R.S., and Zhang, Y. (2004a). Role of histone H2A ubiquitination in Polycomb silencing. Nature *431*, 873–878.

Wang, Y., Wysocka, J., Sayegh, J., Lee, Y.H., Perlin, J.R., Leonelli, L., Sonbuchner, L.S., McDonald, C.H., Cook, R.G., Dou, Y., et al. (2004b). Human PAD4 regulates histone arginine methylation levels via demethylimination. Science *306*, 279–283.

You, A., Tong, J.K., Grozinger, C.M., and Schreiber, S.L. (2001). CoREST is an integral component of the CoREST-human histone deacetylase complex. Proc. Natl. Acad. Sci. USA *98*, 1454–1458.

Zhang, Y., and Reinberg, D. (2001). Transcription regulation by histone methylation: interplay between different covalent modifications of the core histone tails. Genes Dev. *15*, 2343–2360.